Electronic Supplementary Material (ESI) for Journal of Materials Chemistry C.

Electronic Supplementary Information

On the luminescence of $Ti^{4+}$and Eu^{3+} in monoclinic ZrO_2: High performance optical thermometry derived from energy transfer

Guo-Hui Pan[a,b*], Liangliang Zhang[a,b], Huajun Wu[a,b], Xuesong Qu[c], Hao Wu[a,b], Zhendong Hao[a,b], Ligong Zhang[a], Xia Zhang[a,b], Jiahua Zhang[a,b*]

[a]*State Key Laboratory of Luminescence and Applications, Changchun Institute of Optics, Fine Mechanics and Physics, Chinese Academy of Sciences, 3888 Dong Nanhu Road, Changchun 130033, China.*

[b]*Center of Materials Science and Optoelectronics Engineering, University of Chinese Academy of Sciences, Beijing 100049, China*

[c]*Department of Physics, Changchun Normal University, Changchun 130032, China.*

To whom correspondence should be addressed:
guohui.pan@aliyun.com, jhzhang@ciomp.ac.cn

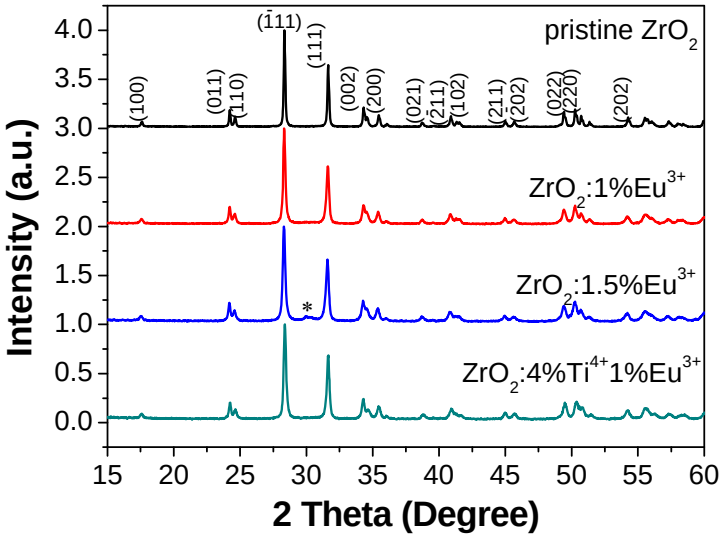

Fig. S1 XRD patterns of several representative samples of pristine ZrO_2, ZrO_2:1%Eu^{3+}, ZrO_2:1.5%$Eu^{3+}$and ZrO_2:4%Ti^{4+},1%Eu^{3+}. The asterisk indicated the presence of trace of t/c-ZrO_2 phase.

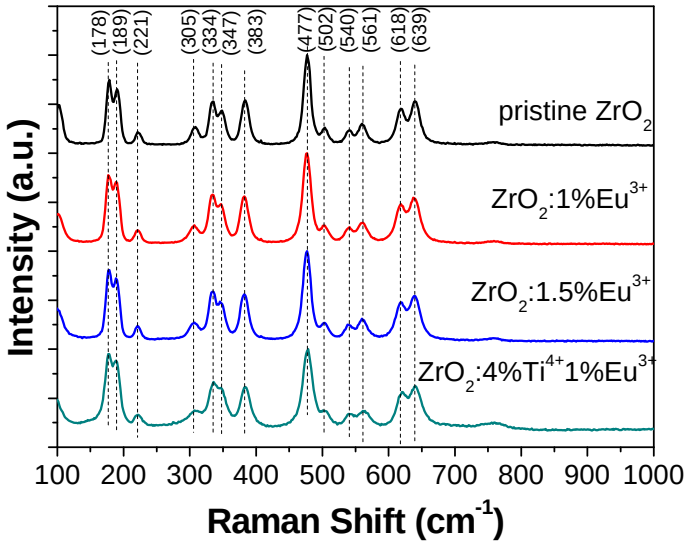

Fig. S2 Raman spectra of several representative samples of pristine ZrO_2, ZrO_2:1%Eu^{3+}, ZrO_2:1.5%$Eu^{3+}$and ZrO_2:4%Ti^{4+},1%Eu^{3+}.

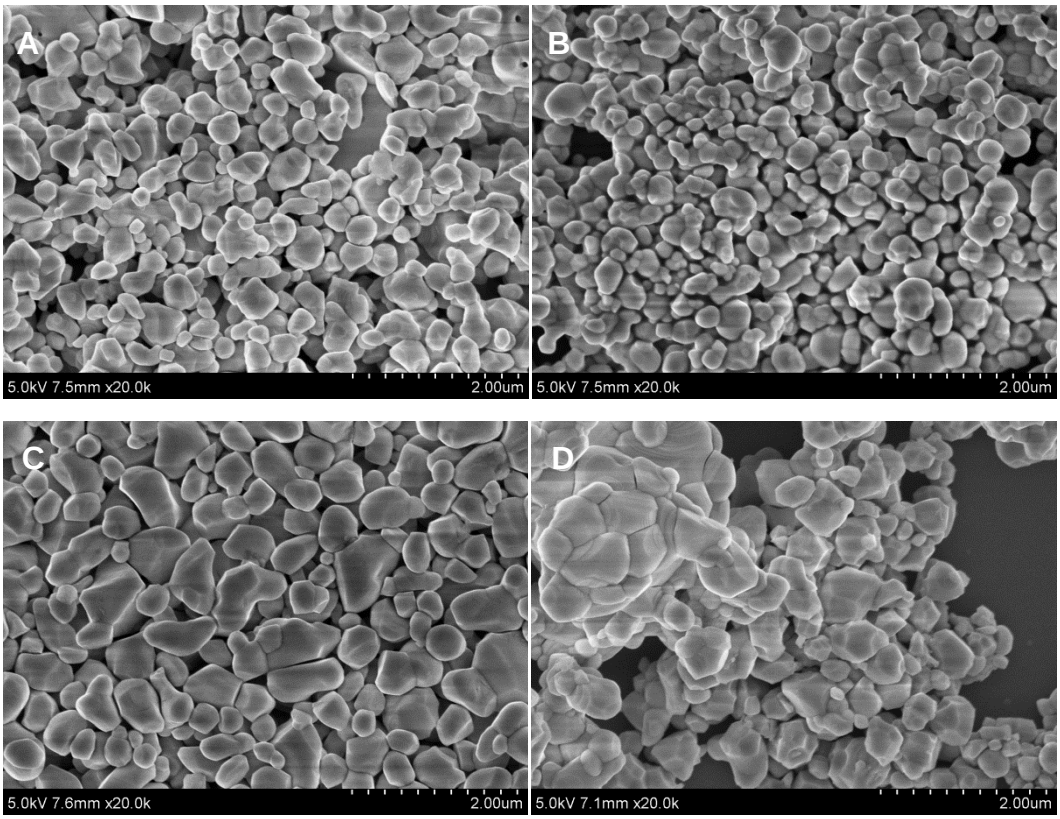

Fig. S3 SEM images of (A) pristine ZrO_2, (B) ZrO_2:1.5%Eu^{3+}, (C) ZrO_2:4%Ti^{4+}, (D) ZrO_2:4%Ti^{4+},1%Eu^{3+} after calcinations at 1300 ^oC for 4 h.

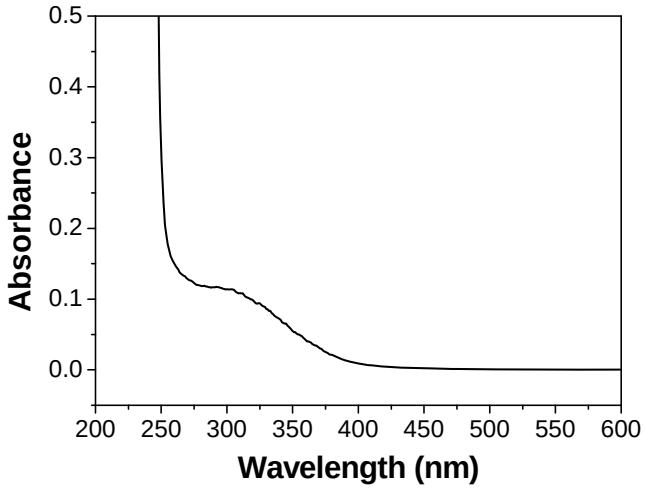

Fig. S4 Zoomed in absorption spectrum of pristine ZrO_2 derived from diffuse reflectance spectrum.

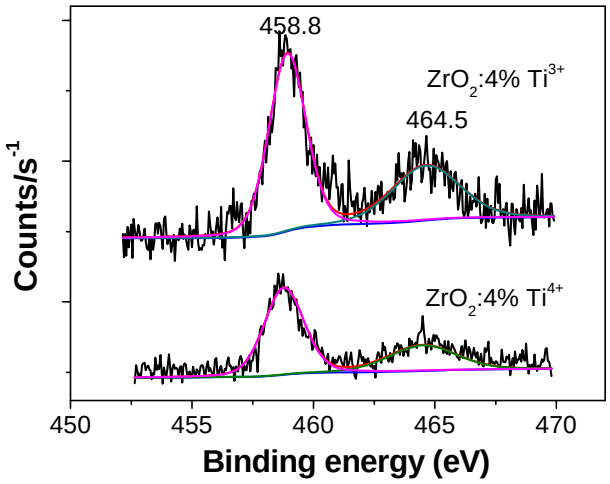

Fig. S5 High resolution XPS scan of Ti 2*p* in m-ZrO_2:4%Ti^{3+} and m-ZrO_2:4%Ti^{4+}. Colored lines indicate the deconvolution results.

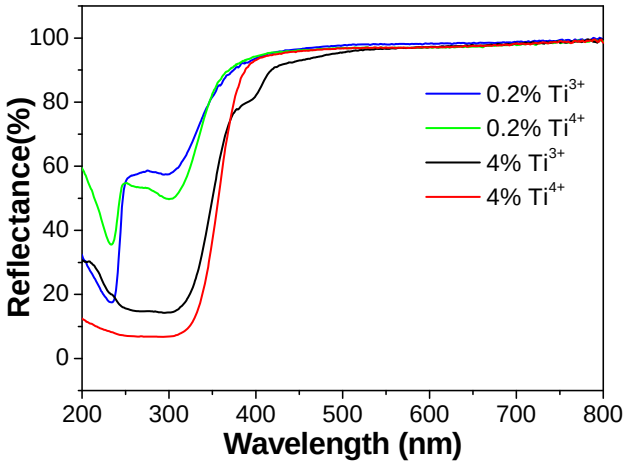

Fig. S6 Diffuse reflectance spectra of samples m-ZrO_2:0.2%Ti^{3+}, m-ZrO_2:0.2%Ti^{4+}, m-ZrO_2:4%Ti^{3+} and m-ZrO_2:4%Ti^{4+}.

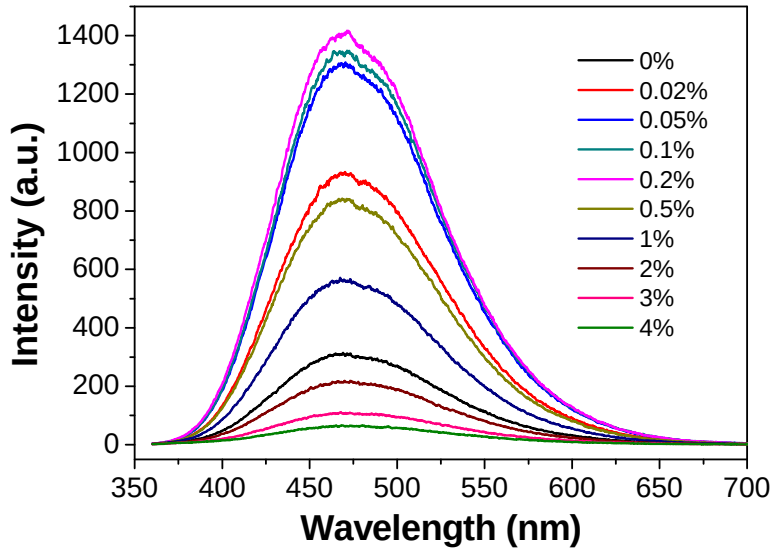

Fig. S7 Emission spectra of pristine ZrO_2 and m-ZrO_2:xTi^{4+} (x= 0.02%, 0.05%, 0.1%, 0.2%, 0.5%, 1%, 2%, 3% and 4%) under 280 nm excitation.

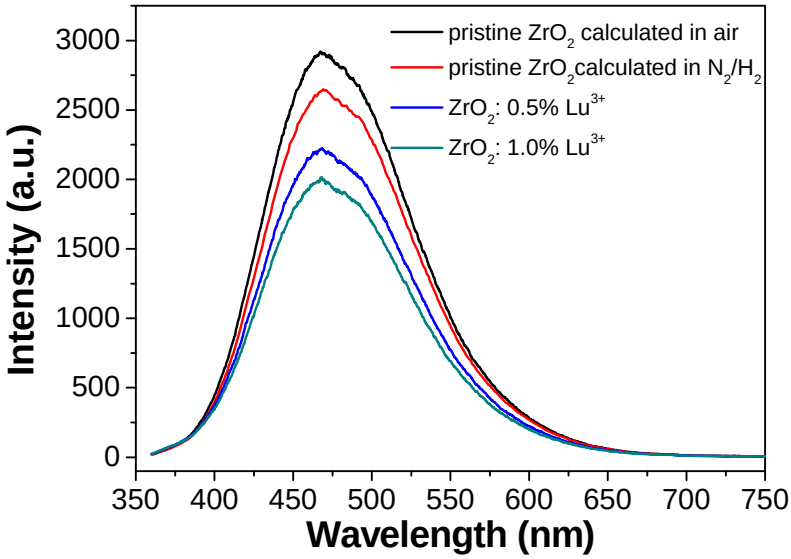

Fig. S8 Emission spectra of pristine ZrO_2 calculated in air, pristine ZrO_2 calculated under reducing atmosphere (N_2/H_2), m-ZrO_2: 0.5%Lu^{3+}, and m-ZrO_2: 1%Lu^{3+} under 280 nm excitation.

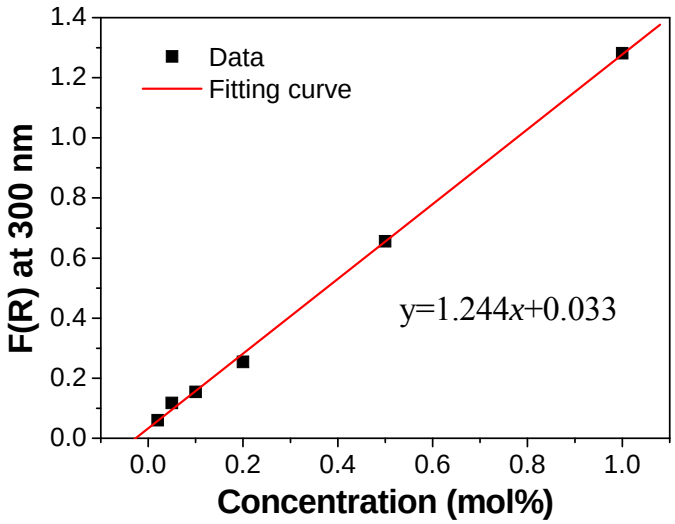

Fig. S9 The F(R) at 300 nm of samples m-ZrO_2:$x$$Ti^{4+}$ (x= 0.02%, 0.05%, 0.1%, 0.2%, 0.5% and 1%) and their linear fitting.

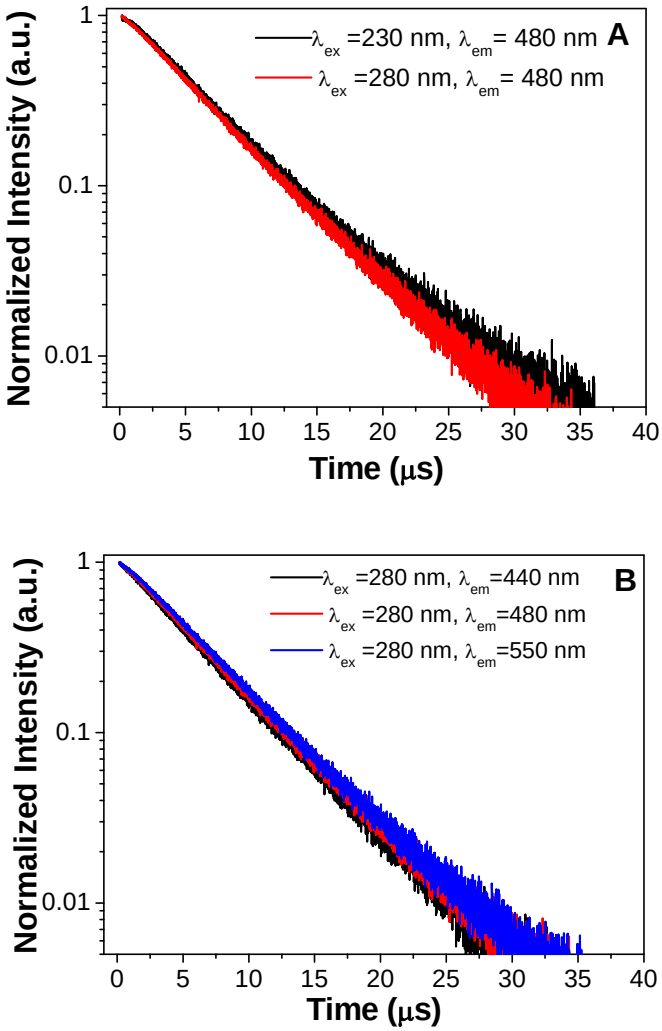

Fig. S10 Fluorescence decays of pristine ZrO_2 at room temperature, (A) excitation at different wavelengths but monitoring the same emission wavelength of 480 nm, (B) excitation at the same wavelength of 280 nm but monitoring the different emission wavelengths.

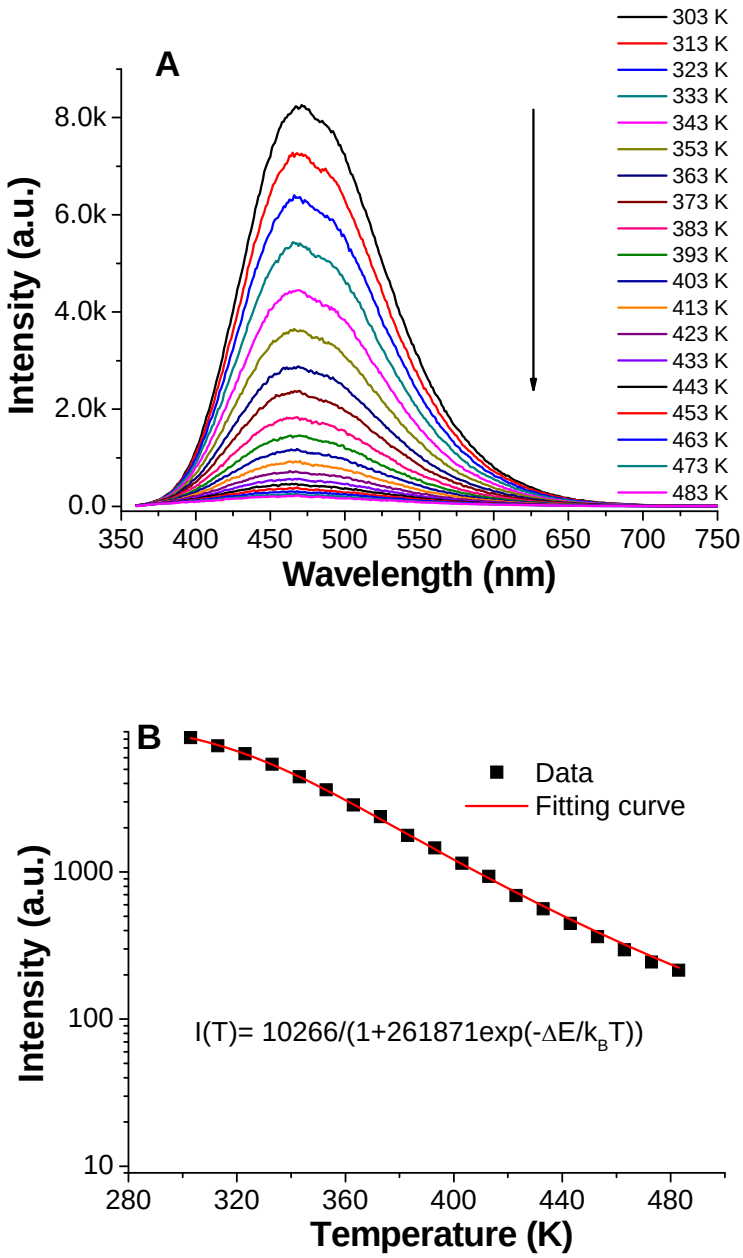

Fig. S11 (A)Temperature-dependent emission spectra of m-ZrO_2:0.2%Ti^{4+} phosphors under 280 nm excitation in the range of 303-483 K. (B)Temperature dependence of the emission intensity (~470 nm) of Ti^{4+}-O^{2-} charge transfer band. The red line is the fitted curve by adopting the Mott-Seitz model,

$$I(T) = \frac{I_0}{1+C\exp\left(\frac{-\Delta E}{k_B T}\right)} ,$$

where I(T) is the temperature-related luminescent intensity, I_0 is the luminescent intensity at T=0 K, C is constant, ΔE is the activation energy of thermal-quenching and k_B is the Boltzmann constant. The extracted activation energies was ~0.36 eV.

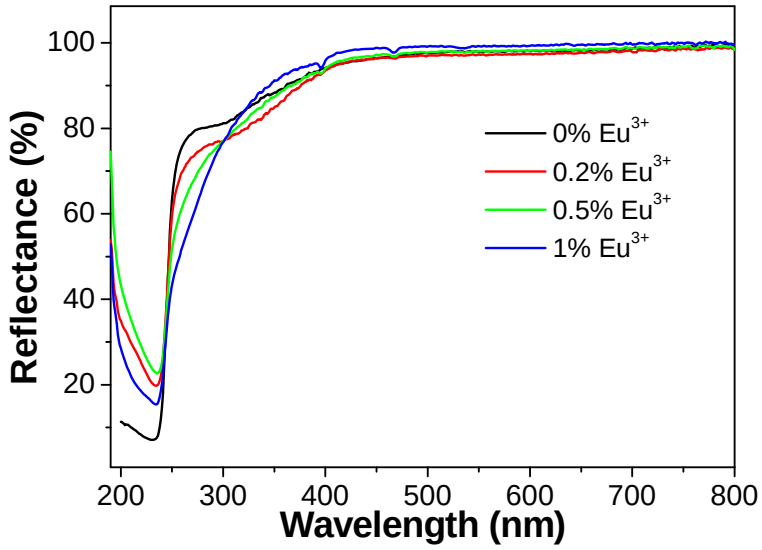

Fig. S12 Diffuse reflectance spectra of (A) m-ZrO_2:*x*Eu^{3+} (x=0, 0.2%, 0.5%, 1%) at room temperature.

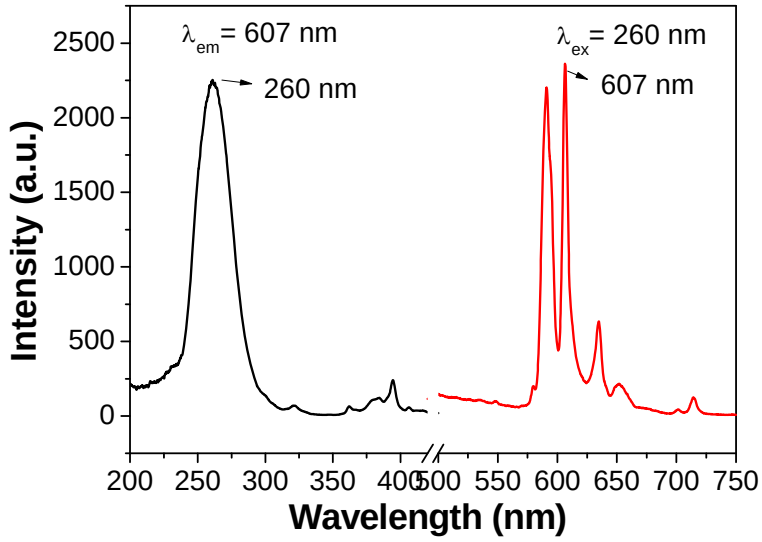

Fig. S13 Excitation and emission spectra of cubic ZrO_2: 0.5% Eu^{3+}, 20%Lu^{3+}. The cubic phase of ZrO_2 was stabilized by massive Lu^{3+} doping.

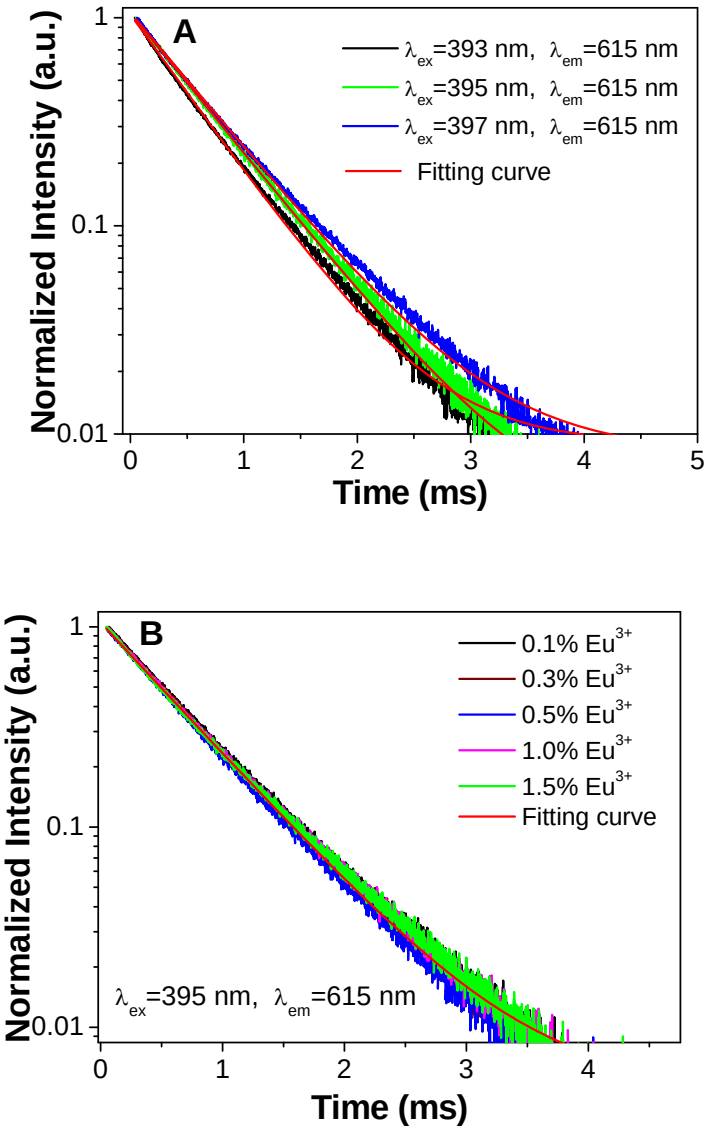

Fig. S14 (A) Fluorescence decays of 615 nm emission of $^5D_0$ level of Eu^{3+} in m-ZrO_2:0.5%Eu^{3+} upon excitation into $^5L_6$ level at different wavelengths; the red lines are the fitted curves for each decay by adopting the single exponential function ($I(t)=\exp(-t/\tau)+C$, where I(t) is the normalized luminescence intensity at time t, C value is background offset, and τ is the decay time for the exponential component.) (B) Fluorescence decays of 615 nm emission of $^5D_0$ level of Eu^{3+} in m-ZrO_2:*x*Eu^{3+} upon excitation into $^5L_6$ level at 395 nm; the red line is a representative fitting curve for m-ZrO_2:1.5%Eu^{3+} by adopting the single exponential decay function.

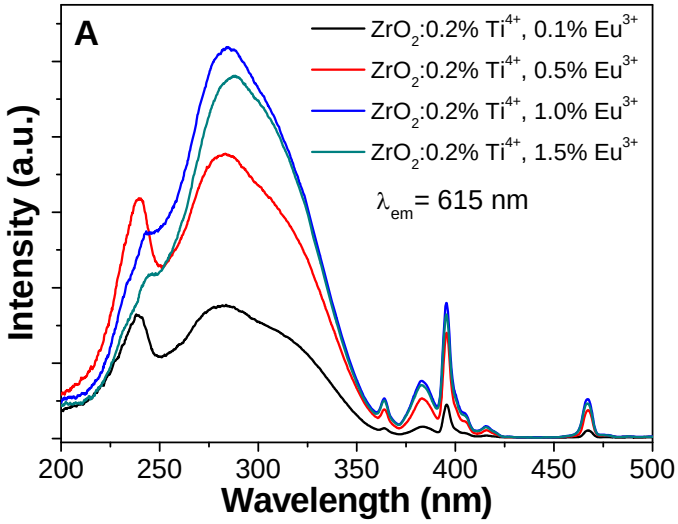

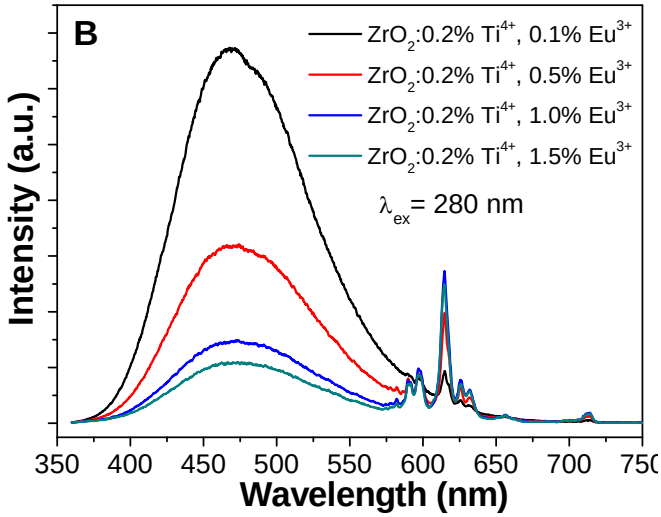

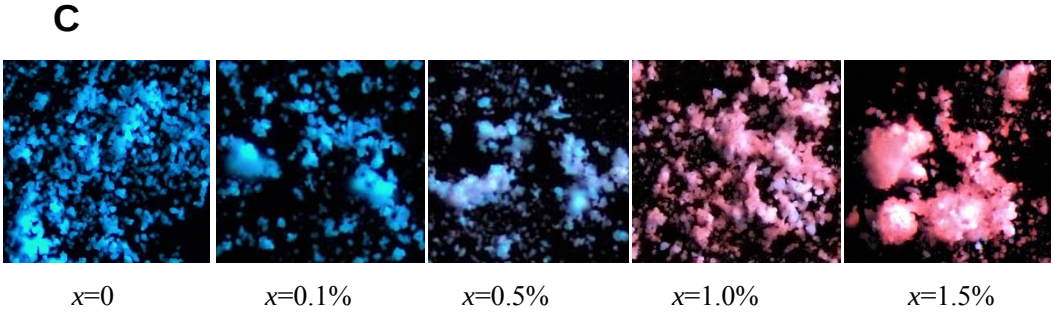

Fig. S15 Excitation (A) and emission (B) spectra of m-ZrO_2:0.2%Ti^{4+},*x*Eu^{3+}. The corresponding excitation and emission wavelengths are indicated in the figures. (C) Fluorescence microscopy images (100×) of samples m-ZrO_2:0.2%Ti^{4+},*x*Eu^{3+} (*x*=0, 0.1%, 0.5%, 1.0%, 1.5%).

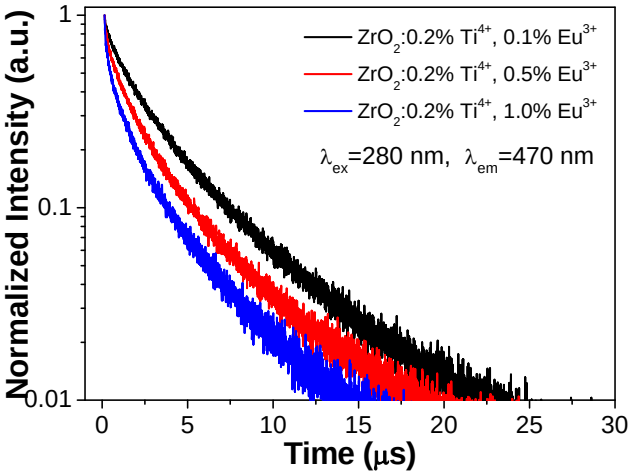

Fig. S16 Fluorescence decays of 470 nm emission of Ti^{4+}-O^{2-} CT band in m-ZrO_2:0.2%Ti^{4+},*x*Eu^{3+} samples upon excitation at 280 nm.

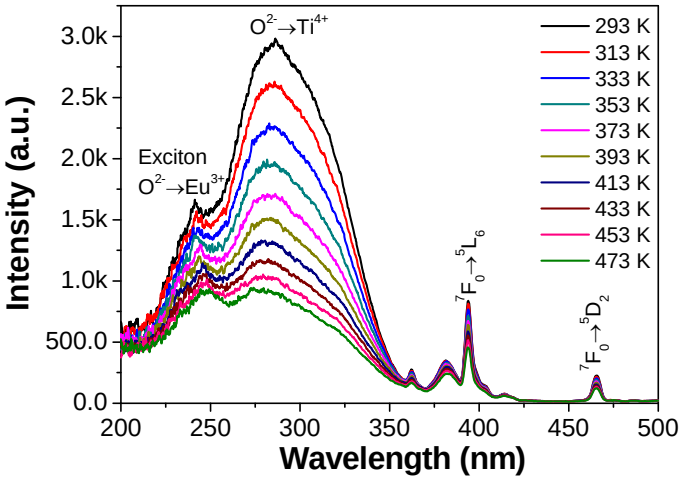

Fig. S17 Temperature-dependent PL excitation spectra of emission of 615 nm for Eu^{3+} in m-ZrO_2:0.2%Ti^{4+},0.5%Eu^{3+} sample in the range of 293-473 K.

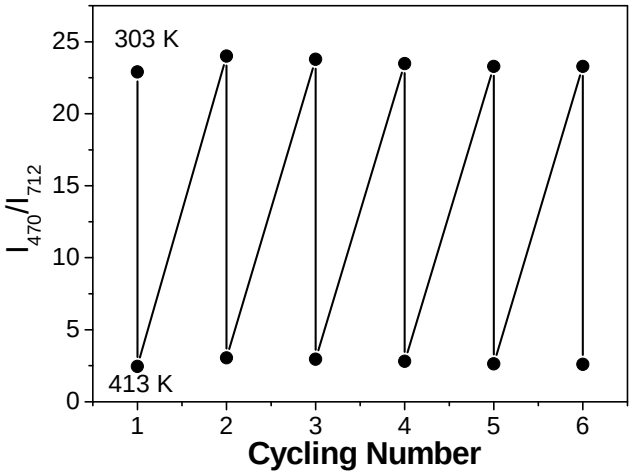

Fig. S18 Temperature-induced switching of FIR between Ti^{4+}-O^{2-} CT emission band (470 nm) and $^5D_0$-$^7F_4$ transition of Eu^{3+} (712 nm) (alternating between 303 K and 413 K).

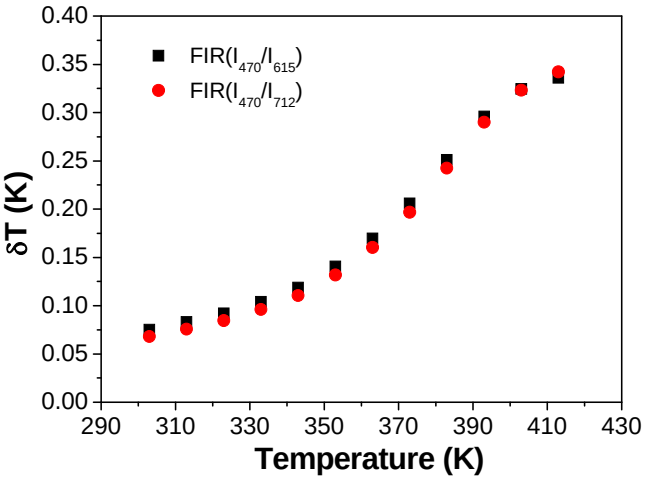

Fig. S19 Temperature resolution δT (303-413 K) of sample ZrO_2:0.2%Ti^{4+}, 0.5%Eu^{3+}

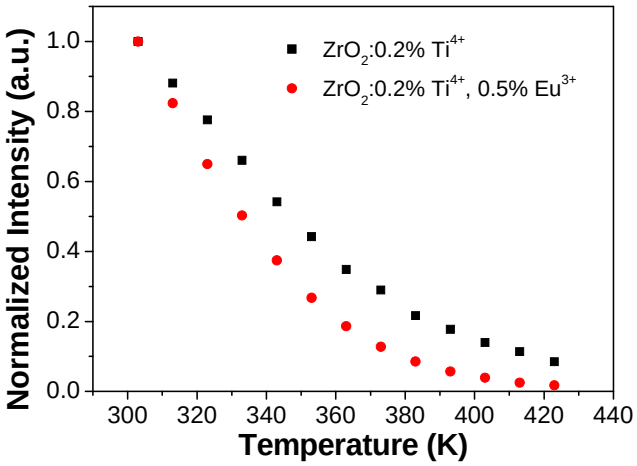

Fig. S20 Temperature dependence of PL of titanium-oxygen complex under excitation of 280 nm in the samples of ZrO_2:0.2%Ti^{4+} and ZrO_2:0.2%Ti^{4+}, 0.5%Eu^{3+}.

Table S1 Temperature sensing performance of some m-ZrO_2:Ti^{4+}, Eu^{3+} samples

Samples	FIR	Function for temperature determination	R^2	maximum S_a (K^{-1})	maximum S_r (%K^{-1})	Temperature range (K)
ZrO_2:0.02%Ti^{4+}, 0.5% Eu^{3+}	$I_{470/615}$	FIR=2524.5391exp(-T/42.9865) -0.01865	0.995	0.032	2.61	323-413
ZrO_2:0.02%Ti^{4+}, 0.5% Eu^{3+}	$I_{470/712}$	FIR=48999.3524exp(-T/41.1557)-0.1418	0.994	0.465	2.60	323-413
ZrO_2:0.1%Ti^{4+},0. 5% Eu^{3+}	$I_{470/615}$	FIR=270.0238exp(-T/63.3660)- 0.2156	0.992	0.031	3.44	323-413
ZrO_2:0.1%Ti^{4+},0. 5% Eu^{3+}	$I_{470/712}$	FIR=5701.6584exp(-T/58.5239) -2.5167	0.994	0.463	3.50	323-413
ZrO_2:0.2%Ti^{4+},1 % Eu^{3+}	$I_{470/615}$	FIR=242.7508exp(-T/49.4536)- 0.00806	0.993	0.011	2.35	303-413
ZrO_2:0.2%Ti^{4+},1 % Eu^{3+}	$I_{470/712}$	FIR=4290.5760exp(-T/47.4524) -0.04197	0.994	0.152	2.24	303-413
ZrO_2:0.2%Ti^{4+},1. 5% Eu^{3+}	$I_{470/615}$	FIR=464.8149exp(-T/42.8730)+ 0.01432	0.994	0.009	2.25	303-413
ZrO_2:0.2%Ti^{4+},1. 5% Eu^{3+}	$I_{470/712}$	FIR=9148.2703exp(-T/40.8114) +0.25325	0.995	0.134	2.34	303-413
ZrO_2:0.5%Ti^{4+},0. 5% Eu^{3+}	$I_{470/615}$	FIR=39.5172exp(-T/89.4250)-0. 2135	0.996	0.019	2.47	283-413
ZrO_2:0.5%Ti^{4+},0. 5% Eu^{3+}	$I_{470/712}$	FIR=624.1698exp(-T/86.3860)- 2.8611	0.996	0.273	2.55	283-413
ZrO_2:0.5%Ti^{4+},1 % Eu^{3+}	$I_{470/615}$	FIR=25.9005exp(-T/65.5866)-0. 0109	0.996	0.006	1.90	273-403
ZrO_2:0.5%Ti^{4+},1 % Eu^{3+}	$I_{470/712}$	FIR=357.8094exp(-T/65.1382)- 0.14275	0.995	0.083	1.91	273-403
ZrO_2:1%Ti^{4+},0.5 % Eu^{3+}	$I_{470/615}$	FIR=62.0047exp(-T/63.6667)+0 .0532	0.997	0.016	1.49	263-413
ZrO_2:1%Ti^{4+},0.5 % Eu^{3+}	$I_{470/712}$	FIR=858.3080exp(-T/61.9855)+ 0.6462	0.997	0.199	1.53	263-413
ZrO_2:1%Ti^{4+},1% Eu^{3+}	$I_{470/615}$	FIR=67.2817exp(-T/47.8563)+0 .03227	0.999	0.006	1.87	263-393
ZrO_2:1%Ti^{4+},1% Eu^{3+}	$I_{470/712}$	FIR=944.6262exp(-T/47.4661)+ 0.45139	0.999	0.076	1.87	263-393
ZrO_2:2%Ti^{4+},0.5 % Eu^{3+}	$I_{470/615}$	FIR=354.4233exp(-T/40.2078)+ 0.08257	0.998	0.013	2.14	263-393
ZrO_2:2%Ti^{4+},0.5 % Eu^{3+}	$I_{470/712}$	FIR=4805.6456exp(-T/39.9012) +1.03835	0.996	0.165	2.17	263-393

Temperature Uncertainty (δT) Estimation

For optical thermometry based on fluorescence intensity ratio (FIR) of two luminescent transitions with intensities of I_1 and I_2,

$$\mathrm{FIR\ (T)} = \frac{\mathrm{I_2}}{\mathrm{I_1}} \qquad (1)$$

in general, the δT values are experimentally determined from the distribution of temperature readouts of a luminescence thermometer when it is at a certain reference temperature.[1] However, recording a set of temperature readouts with statistical significance might not be always feasible.[1] Then, to overcome this limitation, δT can be computed using the following equation:

$$\delta \mathrm{T} = \frac{1}{\mathrm{S_r}} \frac{\delta \mathrm{FIR}}{\mathrm{FIR}} \qquad (2)$$

The estimation of δFIR/FIR can be obtained by considering the uncertainty affecting the intensity measurements. The specific calculation method is as follows[1,2]

$$\frac{\delta \mathrm{FIR}}{\mathrm{FIR}} = \sqrt{\left(\frac{\delta \mathrm{I_1}}{\mathrm{I_1}}\right)^2 + \left(\frac{\delta \mathrm{I_2}}{\mathrm{I_2}}\right)^2} \qquad (3)$$

where $\delta I_i/I_i$ (i=1, 2) is estimated using the single-to-noise ratio (SNR) values. Typically, dividing the readout fluctuations of the baseline by the maximum intensity value allows one to estimate the order of magnitude of $\delta I_i/I_i$.[1] By substituting the estimated value of S_r and δFIR/FIR in equation (2), the quantification of the temperature uncertainty δT is finally achieved.

(1) C. D. S. Brites, A. Millán, L. D. Carlos, Lanthanides in Luminescent Thermometry. In Handbook on the Physics and Chemistry of Rare Earths; Bünzli, J.-C., Pecharsky, V. K., Eds.; Elsevier, 2016; Vol. 49, Chapter 281, pp 339−427.

(2) Q. Wang, M. Liao, Z. Mu, X. Zhang, H. Dong, Z. Liang, J. Luo, Y. Yang, F. Wu, *J. Phys. Chem. C*, 2020, **124**, 886-895.